

WSRC-TR-2002-00407

**Keywords: Aluminosilicate
Evaporator Scaling
Pilot-scale
High Level Waste**

Testing in an Acrylic Evaporator to Aid Understanding of NAS Deposition (U)

David Herman

September 2002

This document was prepared in conjunction with work accomplished under Contract No. DE-AC09-96SR18500 with the U. S. Department of Energy.

DISCLAIMER

This report was prepared as an account of work sponsored by an agency of the United States Government. Neither the United States Government nor any agency thereof, nor any of their employees, makes any warranty, express or implied, or assumes any legal liability or responsibility for the accuracy, completeness, or usefulness of any information, apparatus, product or process disclosed, or represents that its use would not infringe privately owned rights. Reference herein to any specific commercial product, process or service by trade name, trademark, manufacturer, or otherwise does not necessarily constitute or imply its endorsement, recommendation, or favoring by the United States Government or any agency thereof. The views and opinions of authors expressed herein do not necessarily state or reflect those of the United States Government or any agency thereof.

This report has been reproduced directly from the best available copy.

**Available for sale to the public, in paper, from: U.S. Department of Commerce, National Technical Information Service, 5285 Port Royal Road, Springfield, VA 22161,
phone: (800) 553-6847,
fax: (703) 605-6900
email: orders@ntis.fedworld.gov
online ordering: <http://www.ntis.gov/help/index.asp>**

**Available electronically at <http://www.osti.gov/bridge>
Available for a processing fee to U.S. Department of Energy and its contractors, in paper, from: U.S. Department of Energy, Office of Scientific and Technical Information, P.O. Box 62, Oak Ridge, TN 37831-0062,
phone: (865)576-8401,
fax: (865)576-5728
email: reports@adonis.osti.gov**

Summary

As part of the 2H evaporator scaling investigation, a decision was made to construct a small, nominally 5 gallon unit to determine if sufficient data could be obtained at this scale and be representative of the plant system.¹

The acrylic evaporator model was limited to approximately 80 C operational temperature and did not continuously evaporate. Feed solutions used were consistent with earlier deposition simulations² and used a super saturated feed solution.

Some of the major findings for the model testing included:

- The acrylic evaporator system reproduced a deposition pattern similar to that found in the 2H system. This included deposition on the walls and conical area as well as ancillary components such as the lift line and bubbler tube.
- Testing with an air sparger to represent the evaporator steam lance produced an area in the bottom of the conical section that had disproportionately less deposition in a single area of the cone. This cleaner area was similar in appearance to an area observed by inspection of the 2H system.
- The range of mixing rates tested by changing the flow in the sparger showed that deposition was not prevented or reduced significantly. The largest effect was the changing of the location of deposition. Changes in flow patterns altered deposition patterns.
- The acrylic system did not replicate the lack of deposition found on the 2H feed tube. It is believed that the lack of deposition was due in part to the temperature of feed keeping the feed tube cool enough to minimize deposition in combination with a lower density feed providing constant flow across the outside of the tube with low saturation fluid. This “washing” of the feed tube with a lower density feed was

demonstrated. Additionally, the feed to bulk solution temperature difference was much lower in these tests than in the 2H evaporator.

- Of the parameters tested, sparging with air had the greatest influence on mixing in the vessel.
- The general flow pattern observed for the acrylic unit was an upflow in the center following the air bubbles and a downward flow adjacent to the wall. The use of the bubbler has been the dominant factor affecting mixing during testing.

Background

The 242-16H High Level Waste Evaporator processes radioactive waste from the feed tank (Tank 43H), concentrates the waste, and discharges to the concentrate receipt tank (Tank 38H). The processing of Defense Waste Processing Facility Recycle stream includes dissolved and entrained silicon. The silicon reacts with soluble aluminate ion to form an insoluble sodium aluminum silicate. This material has been found in the 2H evaporator.³ The accumulation of solids in the pot prevented evaporator operation for over one year and necessitated the development of a chemical cleaning protocol. Since the cleaning, the evaporator has run without signs of solids buildup. Experimentation continues to understand the accumulation of solids and to prevent reoccurrence.

System description

The system vessel is nominally five gallon capacity. The five gallon unit was selected as a minimum size that would return reasonable and useful results. This sizing was selected based on recommendations from within SRS and outside consultants from MixTech and Holman Engineering.¹ The linear scaling ratio is approximately one-to-seven. Attachment A shows the basis for the scaling of major components. It is accepted that due to the scaling, additional complexities will be found in the actual evaporator that will not be represented in the model.

The tank design is shown in Figure 1. The shape was geometrically scaled to the 2H evaporator. The scaled system included an air lance and a bottom draw to simulate the lift

system in the 2H evaporator. The tank was fed using a small variable flow rate pump.

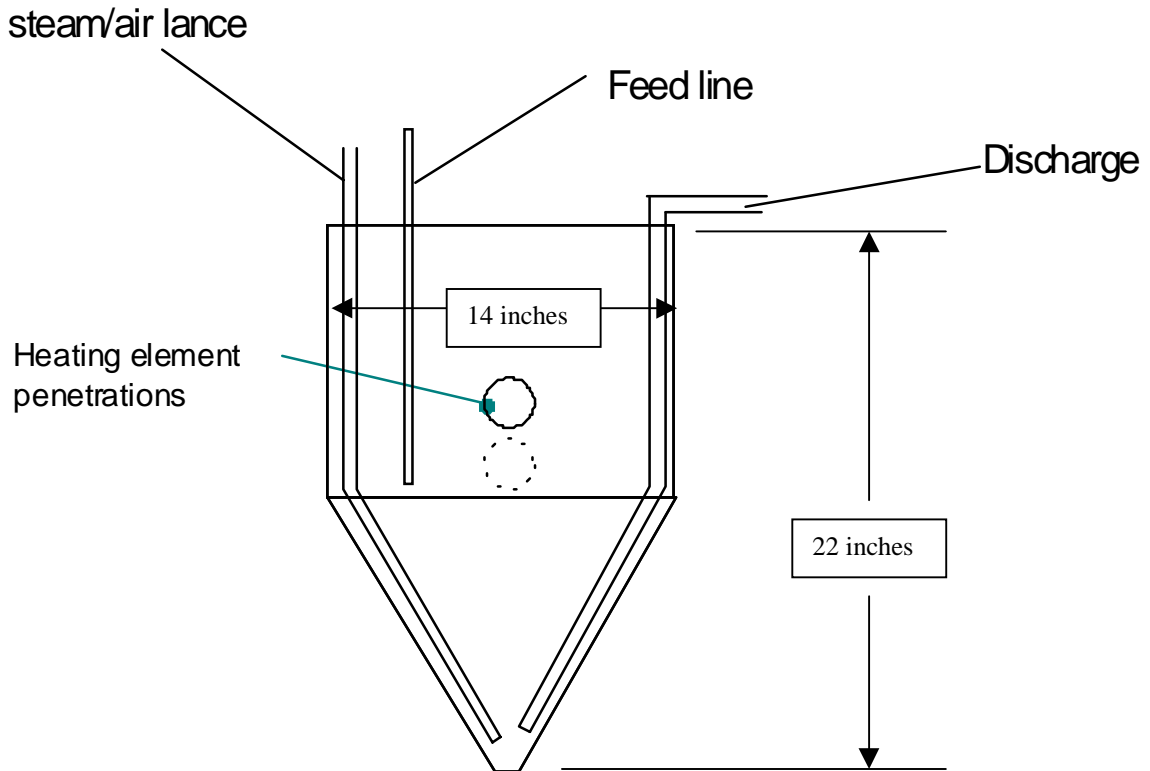


Figure 1. Acrylic tank design.

The vessel tank was constructed in two main sections. The conical section was made by joining several 2-inch slabs of acrylic and then machining the conical shape. This section was then joined to an acrylic pipe forming the right circular cylinder section. The material of construction was cell-cast acrylic sheet. This material allowed for a full view inside of the vessel to observe flow patterns. However, operational temperature was limited due to the material's softening point of 92 C. This restriction prevented the system from achieving sustained evaporation.

Two electric heater elements were used for heat input and were scaled to provide energy input representative of the evaporator steam coils. The heater elements were capable of providing 3 kW each.

The 2H evaporator utilizes a steam lance to promote mixing. A sparger was plumbed in the acrylic model to represent the steam lance in the actual system. Air and water were used as sparging media. Flow rates were scaled on the basis of fluid volume. Calculations show that the contribution of the steam lance to flow is high at the bottom of the cone, but limited at the top. As the steam rises, the cross sectional area of the vessel increases. At the top of the cone, the superficial gas velocity would be very low due to the large cross sectional area. The steam lance will only make a minor contribution of the flow pattern in this area; therefore, an accurate representation of the actual steam lance is limited.⁴ The use of air gave a representation of maximum mixing as would be the case if there was no steam collapse, while water was used to represent a complete steam collapse.

Due to the temperature limitations of the vessel material, a system to remove fluid from the top was used to simulate the loss of material from the system due to evaporation. Removal was taken across the surface instead of a single point withdrawal. Withdrawal rates were scaled using operational data from the 2H evaporator.

The evaporator gravity drain line was replicated using a pump and lift line. Fluid was lifted from the bottom of the vessel and discharged to a surge tank. The surge tank also received fluid from the top withdrawal described above. This tank was then recirculated as feed solution.

Testing

Experiments were run in three phases. Initial testing involved using water as the bulk fluid with the experiments run at room temperature. The objective was to isolate individual components of the mixing including the effect of air sparger flow on the bulk system. The second phase of testing added the heating elements to determine the effect of thermal currents on mixing. The final phase of testing used a supersaturated aluminosilicate solution with the intent to form solids. The intent of these tests was to determine the effect on solid deposition by varying the amount and sources of mixing.

The feed used was 0.1 molar silicon at a ratio of 1:1 with aluminum solution. Hydroxide

concentration was constant at 4 M free hydroxide. Sodium nitrate was used to balance the sodium ion concentration. This feed was consistent with previous studies.^{5,6}

Cold Water Testing

The first set of experiments that was run used an air bubbler to simulate evaporation around the heating coils and evaluate the flow patterns induced by evaporation and the effect of the sparger. Figure 2 shows the air lines used to simulate evaporation.

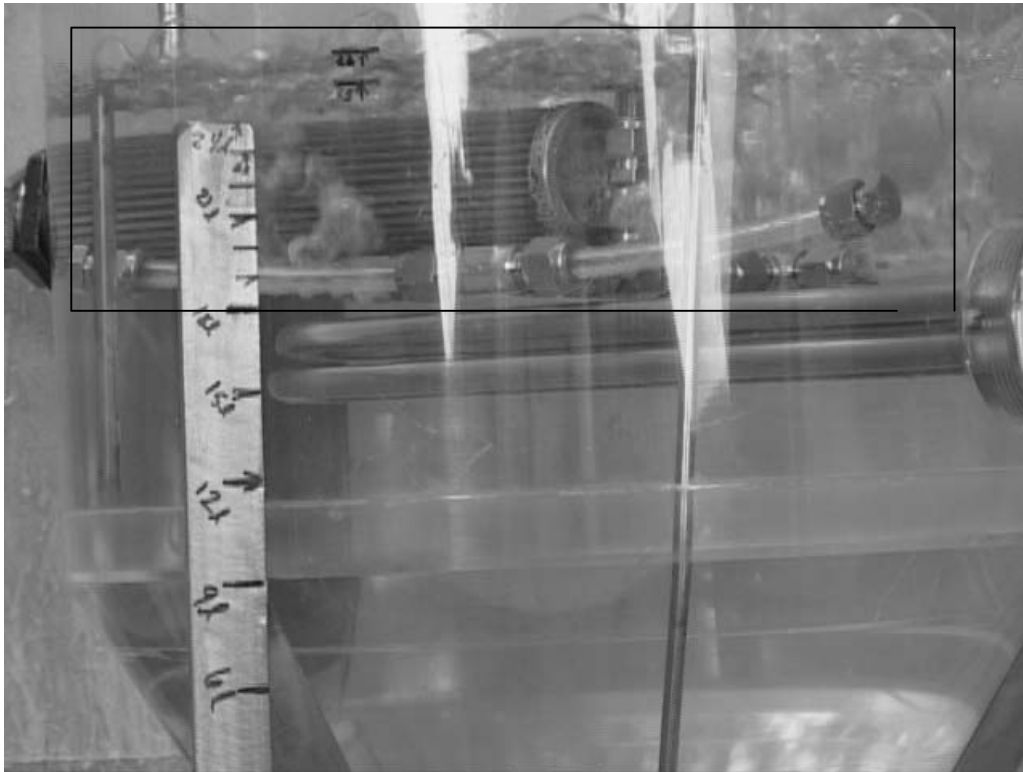


Figure 2. Simulated evaporation using air bubbler.

This testing was done with and without air sparging simulating the steam lance. As predicted, without sparging mixing was at a minimum in the cone region with the only observable pattern being a gradual rising swirl. An upflow was also seen in the immediate vicinity of the simulated heating coils. This flow diminished rapidly as the distance from the heating coils increased. In other words, velocities were greatest directly below and above the simulated evaporation. These velocities fell off very rapidly underneath the heating coils. A very shallow recirculation current was created essentially the depth of the simulated heating

coils with low flows in the rest of the tank.

Cold Water Testing With Air Sparger

The addition of a lower air sparger to simulate the steam lance showed a dramatic increase in mixing in the conical section of the tank. A recirculation current was established encompassing the entire tank. A rapid downward flow was established directly at the wall, and an upward flow was established in the center of the tank. A fairly stagnant region existed halfway between the wall and tank centerline when the sparger was in operation. The sequence of pictures in Figure 3 shows the current flows at the wall as indicated by the dye tracer.

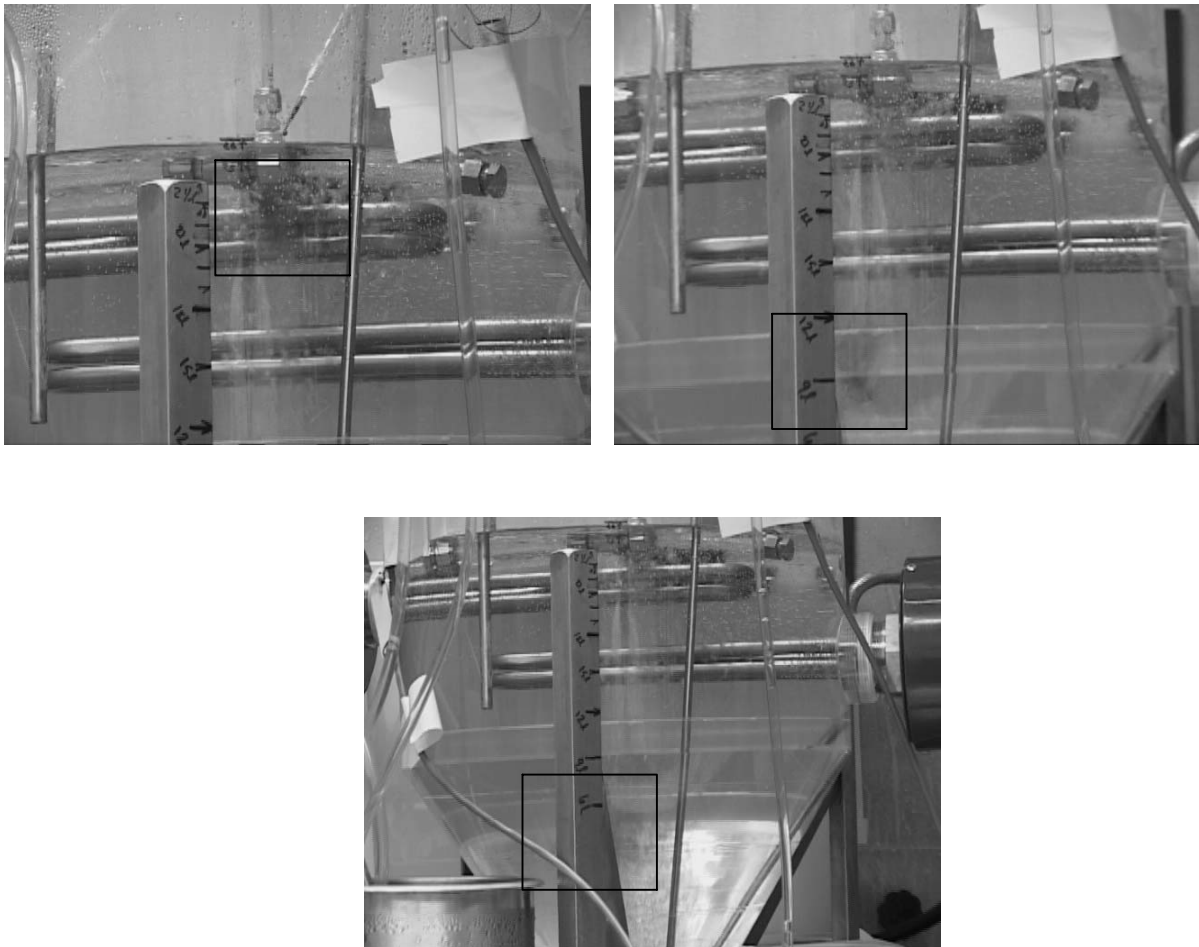


Figure 3. Wall flow with sparger in operation.

The addition of the sparger greatly increased mixing throughout the tank and allowed the

very bottom fluid to be raised to the top center heating coils. A portion of the fluid was removed by simulated evaporation with the remaining fluid circulating out to the wall and then back down to the bottom of the cone.

A tracer was injected at the feed tube outlet to determine the disposition of the feed. The feed was water being added to water at similar temperatures. Therefore, disposition of the feed was totally dependent upon initial velocity provided by the injection pump and the existing currents in the tank. The majority of the feed was caught in the downward wall current and rapidly brought to the bottom of the cone. This is illustrated in Figure 4.

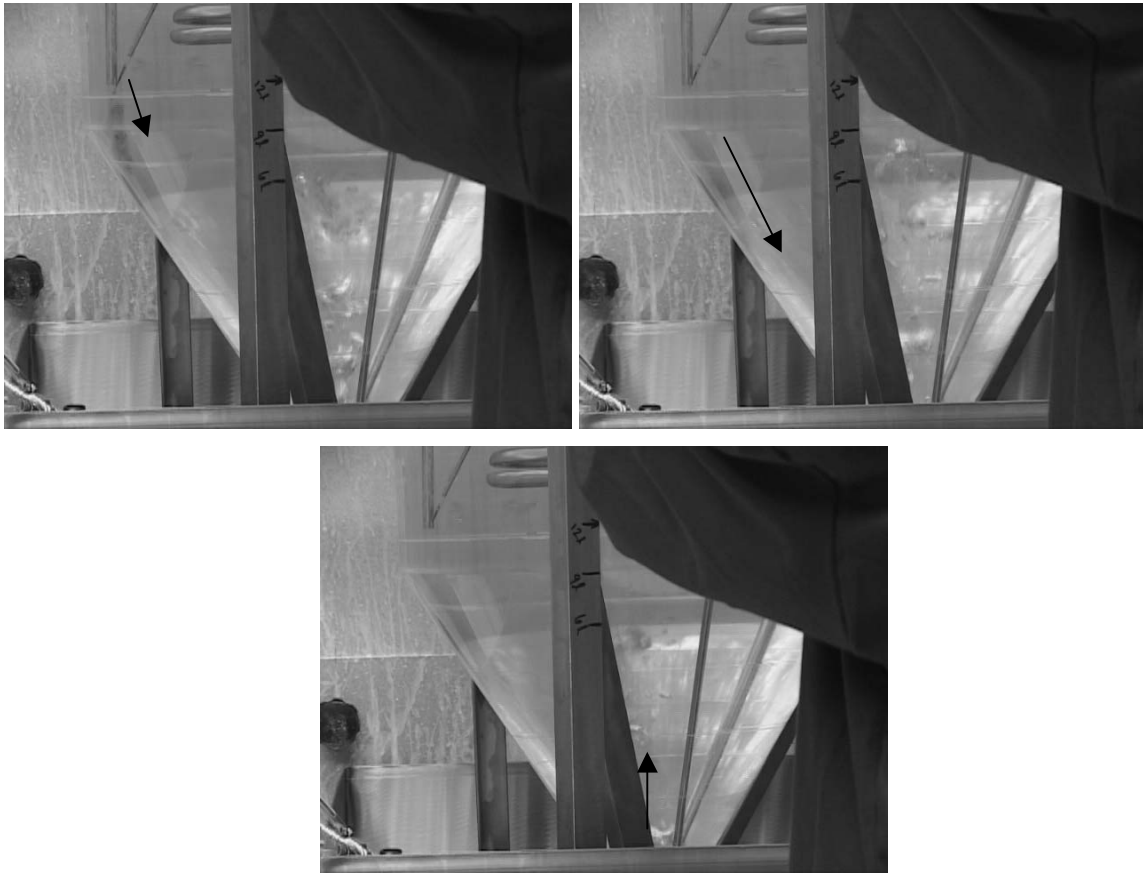


Figure 4. Feed tube flow with feed caught in wall current.

A portion of the feed did not get caught in the wall current and drifted laterally toward the center of the tank until it was caught in the sparger and brought to the surface. This illustrated that the downward flow was localized to the vessel wall. The upward flow from

the sparger was maintained in the center of the vessel. A region of low flow existed between the two flow areas with velocities dropping rapidly outside of the flow currents.

Heated Water Testing

The heating elements were incorporated into the system for this phase of the testing. This allowed for the illustration of the effects of heated fluid. Again, testing was conducted with water and included the removal of fluid across the top to model the loss of material due to evaporation. A bottom draw was also used to simulate the gravity drain line.

In this test a thermal layer was established just under the heating elements. Temperature differences of over 50 C were observed between the surface temperature and the cone bottom temperature. This gradient separated the tank into very distinct regions as illustrated in Figure 5.



Figure 5. Thermal layers in tank with a hot layer at the heating elements, warmer layer due to warm feed, and cool layer at cone bottom.

Three distinct regions formed in this experiment. A separate region formed around the heaters where the temperature was approximately 80 C. A second region formed due to the injection of warm feed. This region was approximately 40 C. The third region in the conical section remained at 25 C. A slow and shallow flow pattern developed around the heating elements. The conical section remained essentially stagnant.

Water Testing Using Sparger and Heating Elements

The sparger was then added to the system to determine the effects on mixing. The addition of the sparger radically changed the flow pattern in the vessel. The thermal layer was immediately disrupted and recirculation in the entire vessel was established. The sparger provided an upflow in the center of the vessel that became the dominant flow driver. A downward flow was also established at the vessel wall.

Low Density Feed with Aluminosilicate Bulk Solution

The initial testing using a light feed solution was to determine possible explanations for the cleanliness of the feed tube in the 2H system. The first test utilized a low density feed added to the bulk caustic solution. The density difference caused the feed to run up the feed tube as illustrated in Figure 6. This action may have contributed to the lack of deposition found on the feed tube in the 2H evaporator.



Figure 6. Low density feed flowing up the side of the feed tube.

50 cc/min Air Sparge

The next test was intended to be a representation of the 2H evaporator under typical operational conditions. The caustic solution was heated to 80 C. Airflow rate to the sparger was 50 cc/min, which was based on scaling of the 2H evaporator operational data.

The flow patterns in the vessel during testing showed a downward flow at the vessel walls and an upward flow in the center of the tank driven by the sparger. The flow pattern is demonstrated in the Figure 7 sequence.

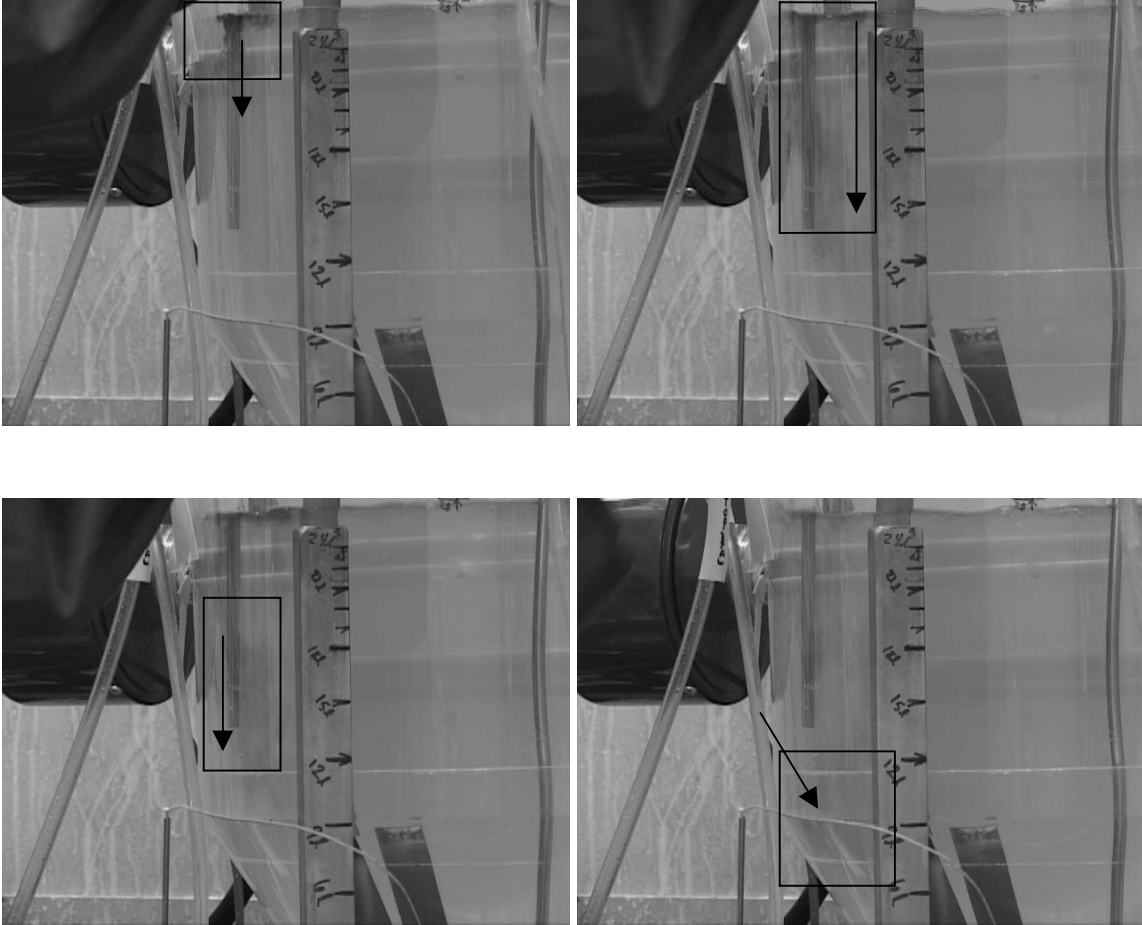


Figure 7. Flow at wall with 50 cc/min sparger.

During testing, the solids appeared to be well distributed throughout the bulk fluid. The liquid temperature from top to bottom was within a few degrees indicating that the tank was reasonably well mixed.

A coating of aluminosilicate solids formed around the vessel and was fairly even across the vessel walls. The vessel with deposition is shown as Figure 8.



Figure 8 Deposition with low air sparger rate.

A small amount of solids had also settled in the bottom of the cone. Solids were found to carry over from the lift line and out of the vessel. There was deposition on the surface of the steel components such as the feed tube, lift line and sparger. Deposition was more pronounced on the top of the heating elements than the bottom. This is illustrated in Figures 9 and 10.

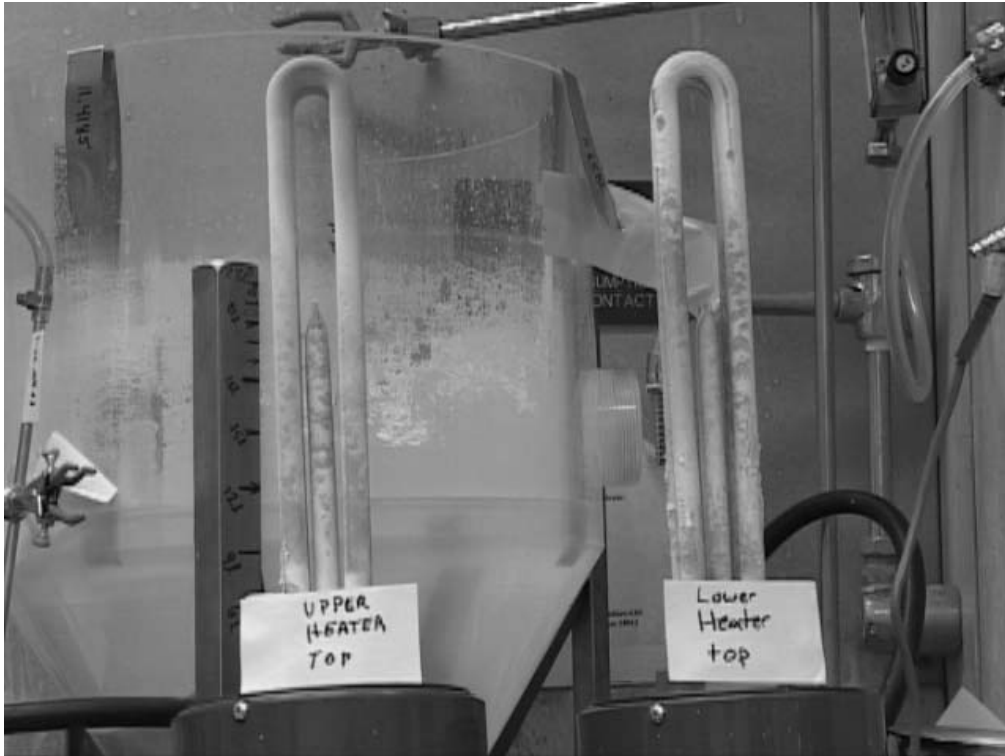


Figure 9. Heating element tops from test with 50cc/min air sparger.



Figure 10. Heating element bottoms from test with 50cc/min air sparger.

As in the later runs, the deposition on the heating elements was the most tenacious. This is believed to be due to the temperature on the surface of the heating elements. Considerable effort was required to clean the deposits from the heating.

High Air Sparge Rate

Tests were then run with an increased air sparger rate. Airflow rate was increased from the previous test to 110 cc/min. As in the previous test, an area in the bottom of the cone near the sparger had a reduced area of deposition as illustrated in Figures 11 and 12.

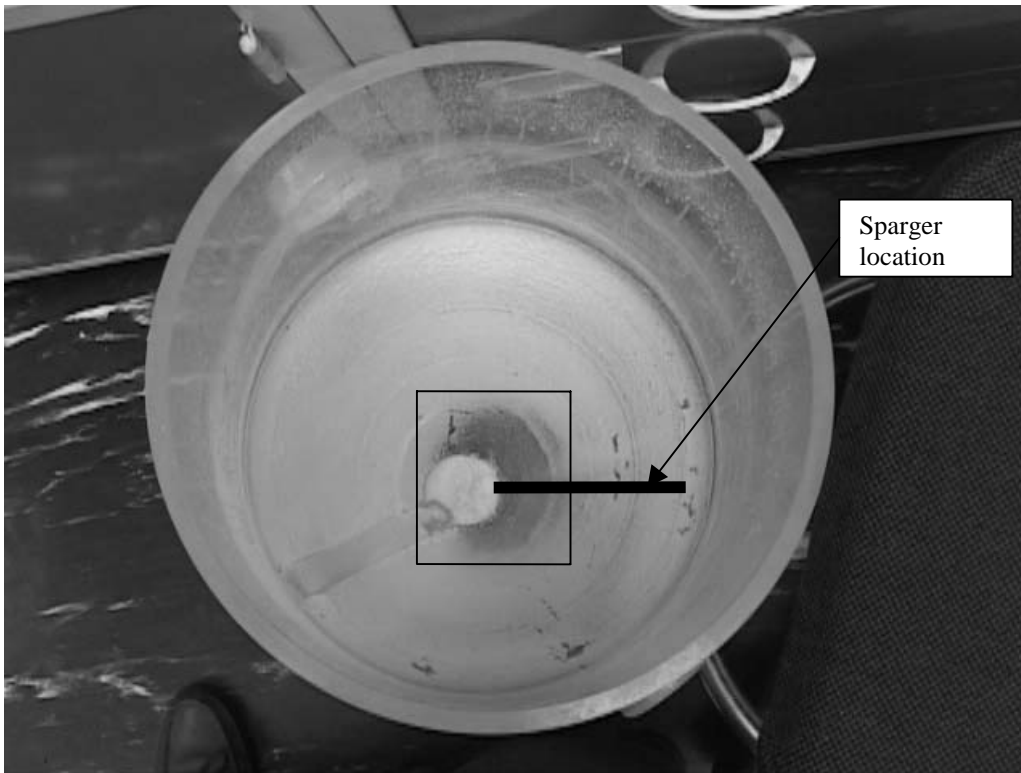


Figure 11. Vessel with high sparger rate showing clean spot.

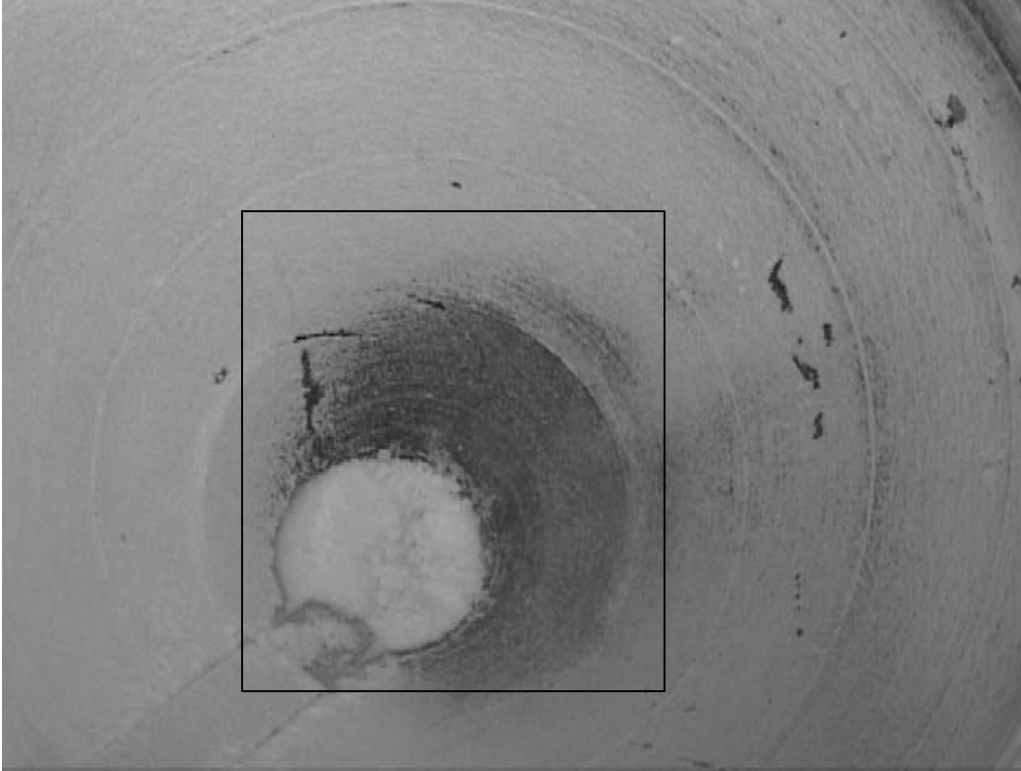


Figure 12. Conical section with area of less deposition.

The general deposition pattern showed a change in location of the solid collection. More deposition compared to the low sparge testing was observed in the conical section of the tank. There appeared to be a shift from even deposition along the walls and conical section to a greater amount of deposition on the conical section. It is believed that this was due to the increased velocity resulting from the higher sparger rate. In this instance, the increasing of mixing did not significantly reduce the amount of deposition but moved the location to areas with reduced velocities and less shear forces. Areas where the components did not sit flush on the vessel wall created dead spots in the fluid flow. These areas collected solids as they formed throughout the test. The cylindrical portion of the vessel showed very little deposition compared with the low sparge test. A side view of the vessel is shown as Figure 13.



Figure 13. Vessel with less deposition on the sidewalls using 110cc/min air sparger.

This is believed to be due to the increase in current flow velocity brought on by the increased sparger airflow. The increased mixing due to the increase in sparger air flow may have provided enough shear to prevent deposition on the vertical surface only to cause an increase in deposition in a transition region of the flow patterns, specifically at the beginning of the conical section.

Sparger flow was insufficient to keep the solids from settling in the bottom of the tank. Solids accumulated in sufficient amounts to rise to the level of the lift line and begin to plug the line. Pluggage was not due to the adhesion of solids to the steel line itself but due to loose accumulation covering over the intake of the line. Large amounts of loose solids were carried over to the surge tank and were of sufficient quantity to adversely affect pumping.

Cleaning of the tank and submerged piping after the experiment proved to be fairly easy with the exception of the heating elements. Most pipes required only wiping off and minimal chemical treatment for cleaning. The most stubborn deposits, other than on the heating

elements, were located on the vessel wall beneath the metal components.

Water Sparger

Tests were run using water in the sparger. This was done to simulate low flow rate due to collapsing steam bubbles. Flow rates were greatly reduced from that of an air sparger. Flow velocities and bulk tank mixing were primarily due to density differences between the low density sparger fluid (1.0 g/cc) and the bulk fluid (1.2 g/cc). Very little mixing occurred in the vessel throughout the test. Solids formed initially in the top section of the tank. Figure 14 shows the layer of solids forming around the heater elements and the limited flow around the heater elements.

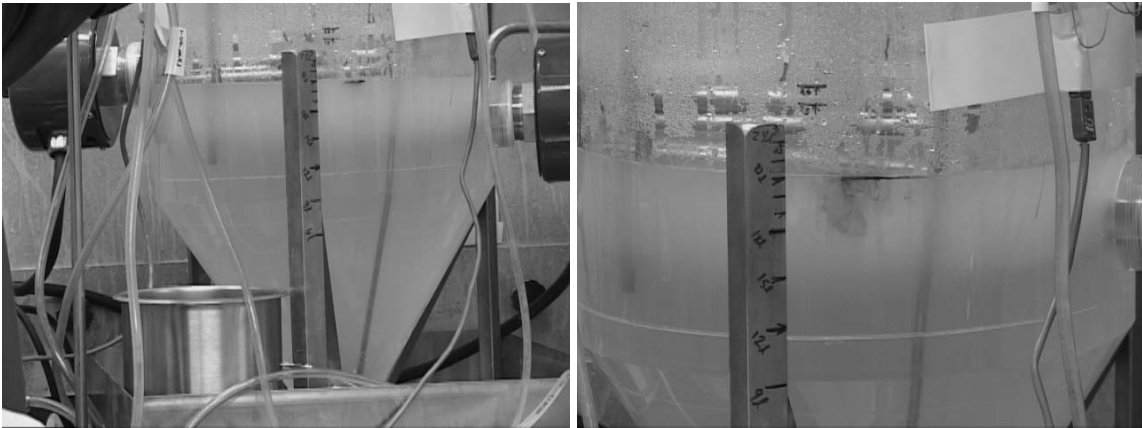


Figure 14. Formation of a layer of solids around the heating elements in a low flow condition.

The flow depth was limited due to the thermal layer caused by the heater elements. It would be expected that these flows would be greater in the actual evaporator due to the increased amount of sustained heat input. A shallow rolling flow was observed from the surface to just beneath the heater elements. Solids slowly began to settle and some mixing did occur due to the sparger. Eventually, suspended solids were visible throughout the tank.

As solids formed, the water sparger would resuspend settling particles until the particles would become too large through agglomeration. This test showed a considerable layer of sediment in the bottom of the cone. Observations during operation showed that much of the

deposition on the cone surface was due to settling. This was confirmed during the post test vessel examination where the solids were very easily removed from the wall, which was noticeably different than previous runs. Further evidence of this was shown just after the vessel was drained and fluid dripped on the vessel wall and washed the solids off. In previous tests, the vessel was lightly sprayed with deionized water and the solids remained.

The solids had a much more tenacious adhesion to the stainless steel piping. Large deposits were formed on all stainless steel lines at the level of the heater elements, the hottest area of the vessel. Solids deposited on the vessel walls at the height of the heating elements. The vessel and deposition patterns are shown in Figure 15.

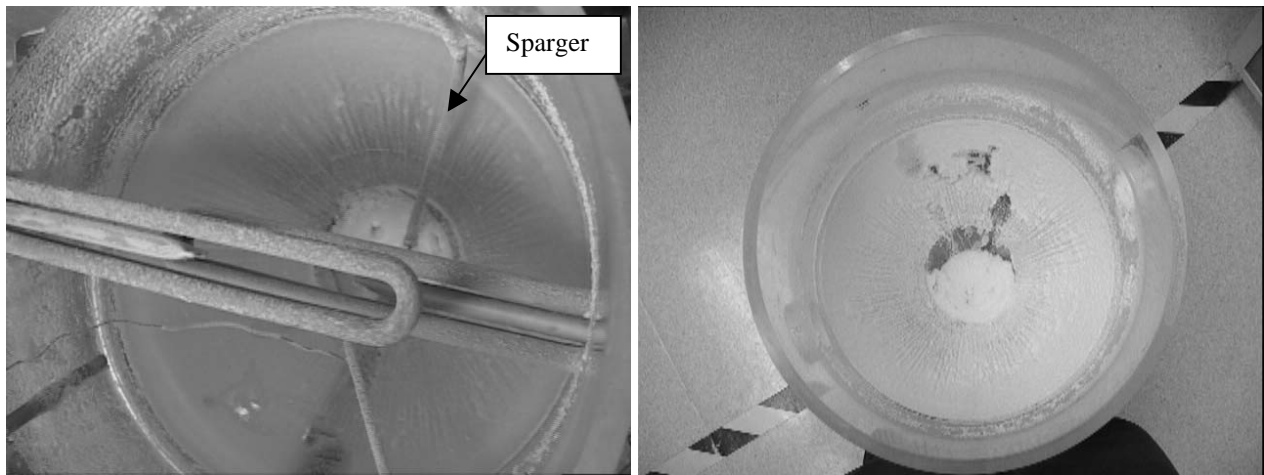


Figure 15. Water sparger vessel with and without components.

Over the different conditions of mixing, very different deposition patterns were observed. When mixing was at a minimum, most of the solids settled. Solid growth was visible on the vessel wall but only in the hottest regions in the vicinity of the heating elements. Loosely attached solids in the lower portions of the vessel were most likely due to the relatively cool surface temperatures.

Feed in Bottom of Cone

An additional test was run in which the feed tube outlet was moved to the bottom of the cone. In this configuration the sparger would aid in feed dispersion. The sparge rate was set at 50

cc/min. The vessel and resulting deposition patterns are shown in Figure 16.

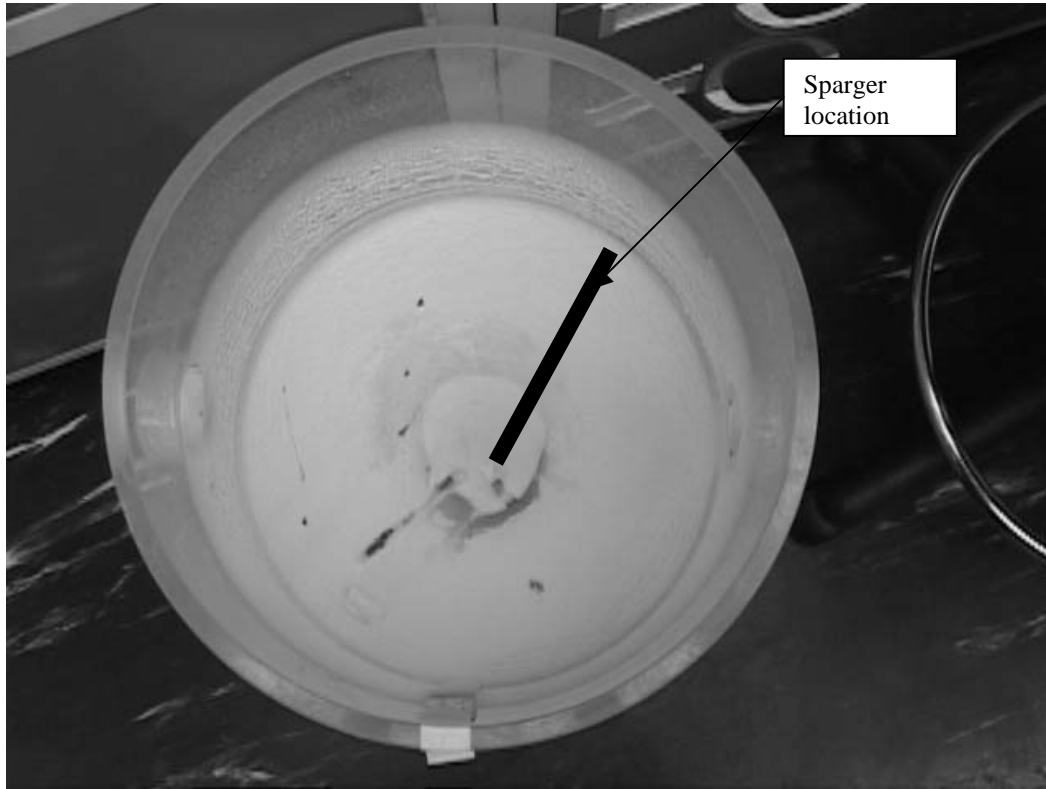


Figure 16. Vessel from the feed-in-cone test.

The results showed an even coating of solids over the vessel area. There is a collection of settled solids in the area that was expected to be clean. For this test, the air sparge position was raised slightly to allow for the feed tube. This small change in position was enough to prevent the wiping of the side wall. The flow rate at the wall was consequently reduced enough such that there was not sufficient velocity to keep the solids suspended though it was sufficient to affect the location of the solids. This resulted in a buildup of solids under the flow in a pattern similar to the cleaner area in previous tests.

A relatively even application of solids was found throughout the vessel. At this scale the mixing did not appear to be reaction limiting. Due to the mixing, surface temperatures were relatively constant throughout the vessel. With an even flow distribution, one would expect the deposition to be relatively constant within the bulk flow pattern.

In a closed loop system that was designed to form solids, the only factor would be the final location of the solids. In this scenario, the increase in mixing and resuspension of solids may have increased deposition on the walls of the vessel by replenishing the solids forming compounds. The increase in wall deposition would reduce the amount of solids that settled in the bottom of the cone.

Conclusions

The acrylic evaporator model was intended to model the aluminosilicate deposition found in the 2H evaporator system. Specifically, the model attempted to model the location of the deposition, and testing was intended to determine if mixing could reduce deposition. The model produced deposition patterns similar to those found in the 2H evaporator and repeatedly reproduced an area of less deposition in the conical section. This area of reduced deposition appears to be the result of the air sparger used in the acrylic model.

Deposition was found to occur more readily on hotter surfaces. In experiments with reduced mixing, a ring of deposition formed on the vessel wall at the height of the heater elements. The most tenacious deposition was on the surface of the heating elements.

Varying the sparger flow rate and using air and water as the sparger fluid tested a wide range of mixing rates. The test using the scaled flow rate of 50 cc/min of air appeared to be the most representative of the actual conditions seen in the 2H evaporator. An evenly distributed deposition pattern was observed with the exception of a small area in the bottom of the conical section, which was fairly clean.

Increased mixing failed to reduce the amount of deposition but did affect its final location. Changes in flow patterns altered deposition patterns including small changes in component positioning. It is expected that altering the flow patterns would more easily change deposition patterns in the conical section. Stagnation areas accumulated solids that proved to be harder to remove than those found on the general wall surface.

The lack of deposition on the feed tube was not reproduced in the acrylic model. It is

speculated that the feed used in testing was too warm to prevent deposition due to recirculation of warm bulk fluid at the same density as feed. Additionally, feed was typically at the same density as the bulk fluid and therefore did not sustain the washing action of the feed tube.

Recommendations

The original intent of using such a small scale for testing was to determine if some of the effects found in the 2H system could be reproduced at a small scale. It has been determined that general trends due to flow effects can be observed at this scale. A larger pilot scale system should show the same effects found here and possibly to a greater degree.

Based on the results of this work, it is recommended to evaluate the value of a larger scale pilot system for continued testing. A larger scale system could potentially be very beneficial as a test bed for evaporator operations. Specifically, testing could be done to support feed qualification and exploring the relationship between feed rate, lift rate and heat flux. The scale of this system would depend on the specific application as defined by the customer. It is unlikely that continued testing would reveal an operational change that would eliminate deposition as was found in the 2H evaporator.

The proposed system should be able to sustain evaporation. The dynamics of the heat addition and concentration of representative feed solution would provide a more realistic representation of the 2H system.

References

1. D. T. Herman, "Task Technical and Quality Assurance Plan for the Acrylic Evaporator Model", WSRC-RP-2002-00268, April 25, 2002.
2. S. W. Rosencrance, D. T. Herman, D. P. Healy, "Formation and Deposition of Aluminosilicates in Support of the 2H Evaporator Fouling Program (U), WSRC-TR-2001-00464, Savannah River Technology Center, Aiken, S. C., September 30, 2001.
3. W. R. Wilmarth, C. J. Coleman, J. C. Hart, and W. T. Boyce, "Characterization of Samples from the 262-16H Evaporator Wall," WSRC-TR-2000-00089, March 20, 2000.
4. D. S. Dickey, MixTech Inc., personal communication, August 27, 2002.
5. L. O. Dworjany, S. C. Smith, a. L. Williams, "Task Technical and Quality Assurance Plan for Evaporator Scaling Dynamics," WSRC-RP-2000-00963, Rev. 0, November 16, 2000.
6. S. W. Rosencrance, D. T. Herman, D. P. Healy, "Task Technical and Quality Assurance Plan for Continuous Aluminosilicate Deposition Testing" WSRC-RP-2001-00731, July 15, 2000.

Evaporator

Geometry

Diameter (O.D.)	96.00 [inches]	
Shell Thickness	0.50 [inches]	
Diameter (I.D.)	95.00 [inches]	
De-Entrainment Chamber (I.D.)	36.00 [inches]	
Cone		
Segment Height	65.56 [inches]	
Top (I.D.)	95.00 [inches]	
Extended Height	82.27 [inches]	
Volume (conical segment)	670.59 [gal.]	
Bottom Head		
Height	16.71 [inches]	
Diameter (I.D.)	19.29 [inches]	
Volume	7.05 [gal.]	
Transition Section		
Area (Avg.)	7,014.08 [sq.in.]	
Height	10.81 [inches]	
Volume (transition section)	328.31 [gal.]	
Heat Exchanger Section		
Width	43.00 [inches]	
Height (Exchanger)	9.25 [inches]	
Length	81.5 [inches]	
Frontal Area (Exchanger)	3,504.50 [sq.in.]	
Circular Area	7,088.22 [sq.in.]	
Cord Length	43.00 [inches]	
Included Angle	27.82 [deg.]	
Sector	1,095.38 [sq.in.]	
Triangle	1,021.25 [sq.in.]	
Segments (2)	148.27 [sq.in.]	
Cross Sectional Area	6,939.95 [sq.in.]	
Height (Exchanger Section)	21.00 [inches]	
Superficial Volume at Heat Exchanger	630.90 [gal.]	
Open Volume	594.59 [gal.]	94.24%
Tubes	233	
O.D.	0.75 [inches]	
Volume	36.32 [gal.]	
Wall	0.083 [inches]	
I.D.	0.584 [inches]	
Flow Area	62.41 [sq.in.]	
Total Superficial Volume	1,636.86 [gal.]	
Estimated Liquid Volume	1,555.02 [gal.]	95.00%

Evaporator

Steam Input	7,000 [lb./hr.]
Heat	6,006,700 [Btu/hr.]
Electric Equivalent	1,761 [kW]
Vapor Evolved	2,765 [cfm]
Liquid Vaporized	12.90 [gpm]
Vapor Velocity Across Exchanger Area	1.89 [ft.sec.]
Lance Steam	200 [lb./hr.]
Vapor Evolved	89 [cfm]
Bottom of Cone (Diameter)	26 [inches]
Bottom of Cone (Area)	530.93 [sq.in.]
Vapor Velocity at Bottom of Cone	0.40 [ft.sec.]
Vapor Velocity at Top of Cone (Theoretical)	0.03 [ft.sec.]

Internals

Feed Pipe (O.D.)	3.50 [inches]
Coil Tubes (O.D.)	1.90 [inches]
Steam Lance (O.D.)	1.90 [inches]
Discharge Pipes (O.D.)	2.38 [inches]
Evaporator Tubes (O.D.)	0.75 [inches]

Flow Rates

Vapor Basis

Evaporator Steam	323.17 [cfm]
Lance Steam	89.33 [cfm]
Vapor Evolved	2,764.83 [cfm]

Liquid Basis

Evaporator Steam	15.86 [gpm]
Lance Steam	0.45 [gpm]
Vapor Evolved	12.90 [gpm]
Liquid Feed	20.03 [gpm]
Liquid Withdrawl	10.01 [gpm]

Evaporator

Scale-Ratio

0.146

Geometry

Diameter (O.D.)	14.00 [inches]
Shell Thickness	0.073 [inches]
Diameter (I.D.)	13.85 [inches]
De-Entrainment Chamber (I.D.)	5.25 [inches]

Cone

Segment Height	9.56 [inches]
Top (I.D.)	13.85 [inches]
Extended Height	12.00 [inches]
Volume (conical segment)	2.08 [gal.]
Bottom Head	
Height	2.44 [inches]
Diameter (I.D.)	2.81 [inches]
Volume	0.022 [gal.]

Transition Section

Area (Avg.)	149.17 [sq.in.]
Height	1.58 [inches]
Volume (transition section)	1.02 [gal.]

Heat Exchanger Section

Width	6.271 [inches]
Height (Exchanger)	1.349 [inches]
Length	11.885 [inches]
Frontal Area (Exchanger)	74.53 [sq.in.]
Circular Area	150.75 [sq.in.]
Cord Length	6.27 [inches]
Included Angle	27.82 [deg.]
Sector	23.30 [sq.in.]
Triangle	21.72 [sq.in.]
Segments (2)	3.15 [sq.in.]

Cross Sectional Area	147.59 [sq.in.]
Height (Exchanger Section)	3.06 [inches]

Superficial Volume at Heat Exchanger	1.96 [gal.]	
Open Volume	1.84 [gal.]	94.24%

Tubes	233
O.D.	0.109 [inches]
Volume	0.113 [gal.]
Wall	0.0121 [inches]
I.D.	0.0852 [inches]
Flow Area	1.33 [sq.in.]

Total Superficial Volume	5.08 [gal.]	
Estimated Liquid Volume	4.82 [gal.]	95.00%

Evaporator

Superficial Velocity

Volume/Volume Flow Rate

Steam Input	149 [lb./hr.]	22 [lb./hr.]
Heat	127,747 [Btu/hr.]	18,630 [Btu/hr.]
Electric Equivalent	37 [kW]	5 [kW]
Vapor Evolved	58.8 [cfm]	8.58 [cfm]
Liquid Vaporized	0.27 [gpm]	0.04 [gpm]
Vapor Velocity Across Exchanger Area	1.89 [ft.sec.]	0.28 [ft.sec.]
Lance Steam	41 [lb./hr.]	6 [lb./hr.]
Vapor Evolved	1.90 [cfm]	0.28 [cfm]
Bottom of Cone (Diameter)	3.79 [inches]	3.79 [inches]
Bottom of Cone (Area)	11.29 [sq.in.]	11.29 [sq.in.]
Vapor Velocity at Bottom of Cone	0.404 [ft.sec.]	0.059 [ft.sec.]
Vapor Velocity at Top of Cone (Theoretical)	0.030 [ft.sec.]	0.004 [ft.sec.]

Internals

Feed Pipe (O.D.)	0.510 [inches]
Coil Tubes (O.D.)	0.277 [inches]
Steam Lance (O.D.)	0.277 [inches]
Discharge Pipes (O.D.)	0.346 [inches]
Evaporator Tubes (O.D.)	0.109 [inches]

Flow Rates

Vapor Basis

Evaporator Steam	6.87 [cfm]	1.00 [cfm]
Lance Steam	1.90 [cfm]	0.28 [cfm]
Vapor Evolved	58.80 [cfm]	8.58 [cfm]

Liquid Basis

Evaporator Steam	0.337 [gpm]	0.049 [gpm]
Lance Steam	0.093 [gpm]	0.014 [gpm]
Vapor Evolved	0.274 [gpm]	0.040 [gpm]
Liquid Feed	0.551 [gpm]	0.080 [gpm]
Liquid Withdrawl	0.276 [gpm]	0.040 [gpm]

Evaporator

Scale-Ratio

0.188

Geometry

Diameter (O.D.)	18.00 [inches]
Shell Thickness	0.094 [inches]
Diameter (I.D.)	17.81 [inches]
De-Entrainment Chamber (I.D.)	6.75 [inches]

Cone

Segment Height	12.29 [inches]
Top (I.D.)	17.81 [inches]
Extended Height	15.43 [inches]
Volume (conical segment)	4.42 [gal.]
Bottom Head	
Height	3.13 [inches]
Diameter (I.D.)	3.62 [inches]
Volume	0.046 [gal.]

Transition Section

Area (Avg.)	246.59 [sq.in.]
Height	2.03 [inches]
Volume (transition section)	2.16 [gal.]

Heat Exchanger Section

Width	8.063 [inches]
Height (Exchanger)	1.734 [inches]
Length	15.281 [inches]
Frontal Area (Exchanger)	123.21 [sq.in.]
Circular Area	249.20 [sq.in.]
Cord Length	8.06 [inches]
Included Angle	27.82 [deg.]
Sector	38.51 [sq.in.]
Triangle	35.90 [sq.in.]
Segments (2)	5.21 [sq.in.]
Cross Sectional Area	243.98 [sq.in.]
Height (Exchanger Section)	3.94 [inches]
Superficial Volume at Heat Exchanger	4.16 [gal.]
Open Volume	3.92 [gal.]
Tubes	233
O.D.	0.141 [inches]
Volume	0.239 [gal.]
Wall	0.0156 [inches]
I.D.	0.1095 [inches]
Flow Area	2.19 [sq.in.]

Total Superficial Volume

10.79 [gal.]

Estimated Liquid Volume

10.25 [gal.]

94.24%

95.00%

Evaporator

Superficial Velocity

Volume/Volume Flow Rate

Steam Input	246 [lb./hr.]	46 [lb./hr.]
Heat	211,173 [Btu/hr.]	39,595 [Btu/hr.]
Electric Equivalent	62 [kW]	12 [kW]
Vapor Evolved	97.2 [cfm]	18.23 [cfm]
Liquid Vaporized	0.45 [gpm]	0.09 [gpm]
Vapor Velocity Across Exchanger Area	1.89 [ft.sec.]	0.36 [ft.sec.]
Lance Steam	68 [lb./hr.]	13 [lb./hr.]
Vapor Evolved	3.14 [cfm]	0.59 [cfm]
Bottom of Cone (Diameter)	4.88 [inches]	4.88 [inches]
Bottom of Cone (Area)	18.67 [sq.in.]	18.67 [sq.in.]
Vapor Velocity at Bottom of Cone	0.404 [ft.sec.]	0.076 [ft.sec.]
Vapor Velocity at Top of Cone (Theoretical)	0.030 [ft.sec.]	0.006 [ft.sec.]

Internals

Feed Pipe (O.D.)	0.656 [inches]
Coil Tubes (O.D.)	0.356 [inches]
Steam Lance (O.D.)	0.356 [inches]
Discharge Pipes (O.D.)	0.445 [inches]
Evaporator Tubes (O.D.)	0.141 [inches]

Flow Rates

Vapor Basis

Evaporator Steam	11.36 [cfm]	2.13 [cfm]
Lance Steam	3.14 [cfm]	0.59 [cfm]
Vapor Evolved	97.20 [cfm]	18.23 [cfm]

Liquid Basis

Evaporator Steam	0.558 [gpm]	0.105 [gpm]
Lance Steam	0.154 [gpm]	0.029 [gpm]
Vapor Evolved	0.453 [gpm]	0.085 [gpm]
Liquid Feed	0.911 [gpm]	0.171 [gpm]
Liquid Withdrawl	0.456 [gpm]	0.085 [gpm]